Journal Pre-proofs

Silymarin-albumin nanoplex: preparation and its potential application as an antioxidant in nervous system *in vitro* and *in vivo*

Mohammad Javad Sohrabi, Ahmad-Reza Dehpour, Farnoosh Attar, Anwarul Hasan, Nahid Mohammad-Sadeghi, Ali Akbar Meratan, Falah Mohammad Aziz, Abbas Salihi, Mudhir Sabir Shekha, Keivan Akhtari, Koorosh Shahpasand, Seyed Mohammad Masood Hojjati, Majid Sharifi, Ali Akbar Saboury, Seyed Mahdi Rezayat, Seyyedeh Elaheh Mousavi, Mojtaba Falahati

PII: S0378-5173(19)30869-5
DOI: https://doi.org/10.1016/j.ijpharm.2019.118824
Reference: IJP 118824

To appear in: *International Journal of Pharmaceutics*

Received Date: 7 August 2019
Revised Date: 5 October 2019
Accepted Date: 25 October 2019

Please cite this article as: M.J. Sohrabi, A-R. Dehpour, F. Attar, A. Hasan, N. Mohammad-Sadeghi, A.A. Meratan, F.M. Aziz, A. Salihi, M.S. Shekha, K. Akhtari, K. Shahpasand, S.M.M. Hojjati, M. Sharifi, A.A. Saboury, S.M. Rezayat, S.E. Mousavi, M. Falahati, Silymarin-albumin nanoplex: preparation and its potential application as an antioxidant in nervous system *in vitro* and *in vivo*, *International Journal of Pharmaceutics* (2019), doi: https://doi.org/10.1016/j.ijpharm.2019.118824

Silymarin-albumin nanoplex: preparation and its potential application as an antioxidant in nervous system *in vitro* and *in vivo*

Mohammad Javad Sohrabi [1], Ahmad-Reza Dehpour [1], Farnoosh Attar [2], Anwarul Hasan [3, 4], Nahid Mohammad-Sadeghi [5], Ali Akbar Meratan [5], Falah Mohammad Aziz [6], Abbas Salihi [6, 7], Mudhir Sabir Shekha [6, 8], Keivan Akhtari [9], Koorosh Shahpasand [10], Seyed Mohammad Masood Hojjati [11], Majid Sharifi[12], Ali Akbar Saboury [13], Seyed Mahdi Rezayat [1,14*], Seyyedeh Elaheh Mousavi [1*], Mojtaba Falahati [12*]

[1]Department of Pharmacology, School of Medicine, Tehran University of Medical Sciences, Tehran, Iran
[2]Department of Biology, Faculty of Food Industry & Agriculture, Standard Research Institute (SRI), Karaj, Iran
[3]Department of Mechanical and Industrial Engineering, College of Engineering, Qatar University, Doha 2713, Qatar
[4] Biomedical Research Center, Qatar University, Doha 2713, Qatar.
[5] Department of Biological Sciences, Institute for Advanced Studies in Basic Sciences (IASBS), Zanjan, Iran
[6]Department of Biology, College of Science, Salahaddin University-Erbil, Kurdistan Region, Iraq
[7] Department of Medical Analysis, Faculty of Science, Tishk International University, Erbil, Iraq.
[8] Department of Pathological Analysis, College of Science, Knowledge University, Erbil 074016, Kurdistan Region, Iraq
[9] Department of Physics, University of Kurdistan, P.O. Box 416, Sanandaj, Iran
[10] Royan Institute for Stem Cell Biology and Technology (RI-SCBT), Tehran, Iran
[11] Department of Neurology, Babol University of Medical Sciences, Babol, Iran
[12] Department of Nanotechnology, Faculty of Advanced Science and Technology, Tehran Medical Sciences, Islamic Azad University, Tehran, Iran
[13] Institute of Biochemistry and Biophysics, University of Tehran, Tehran, Iran
[14] Department of Medical Nanotechnology, School of Advanced Technologies in Medicine, Tehran University of Medical Sciences, Tehran, Iran

Corresponding authors:

Seyed Mahdi Rezayat, Email: rezayat@tums.ac.ir

Seyyedeh Elaheh Mousavi, Email: semousavi@sina.tums.ac.ir

Mojtaba Falahati, Email: mojtaba.falahati@alumni.ut.ac.ir

Abstract

In this study, we formulated silymarin-HSA nanoplex and assayed its ability to reduce LPS-induced toxicity *in vitro* and *in vivo*. Silymarin molecules were encapsulated into HSA nanoplex and the loading efficiency and characterization of fabricated nanoplex were performed by using HPLC, TEM, SEM, DLS, FTIR analysis, and theoretical studies. Afterwards, their protective effect against LPS (20 µg/ml) -induced toxicity in SH-SY5Y cells was investigated by MTT, ROS, and apoptosis assays. For *in vivo* experiments, rats were pre-treated with either silymarin or silymarin -HSA nanoplex (200 mg/kg) orally for 3 days and at third day received LPS by IP at a dose of 0.5 mg/kg, 150 min before scarification followed by SOD and CAT activity assay. The formulation of silymarin-HSA nanoplex showed a spherical shape with an average diameter between 50 nm to 150 nm, hydrodynamic radius of 188.3 nm, zeta potential of -26.6 mV, and a drug loading of 97.3%. In LPS-treated cells, pretreatments with silymarin-HSA noncomplex recovered the cell viability and decreased the ROS level and corresponding apoptosis more significantly than free silymarin. In rats, it was also depicted that, silymarin-HSA noncomplex can increase the SOD and CAT activity in brain tissue at LPS-triggered oxidative stress model more significantly than free counterpart. Nanoformulation of silymarin improved its capability to reduce LPS-induced oxidative stress by restoring cell viability and elevation of SOD and CAT activity *in vitro* and *in vivo*, respectively. Therefore, formulation of silymarin may hold a great promise in the field of antioxidant agent development.

Keywords: silymarin, albumin, nanoplex, antioxidant, *in vitro*, *in vivo*

1. Introduction

In spite of the application of herbs in pharmaceutical and cosmetic industries, the poor absorption and poor bioavailability after oral administration may affect their physiological properties [1-3]. Indeed, difficulties regarding poor solubility, adsorption and stability inhibit the bioavailability, bioactivity and function of the herbs [4-6]. Hence, enhancing the solubility and desired therapeutic impacts of herbs will need a functional delivery system.

To overcome these imperfections, it has been well documented that the nanoformulation of herbs enhanced their solubility, tissue distribution, and bioactivity [7]. Indeed, the nanosized particles of polyphenols followed by higher surface area may lead to an increase in the kinetic of drug release and enhanced absorption pursued to improved bioactivity in lesser dose of drug. Nano-capsulation by using polymers [8, 9], liposome [10, 11] and albumin [12, 13] has been suggested pointing at both enhancing their bioavailability and stability. Albumin NPs proffer a number of advantages, specifically increasing the bioavailability, stability and function of molecules. For example, Bonoli-Carbognin et al., [14] revealed that albumin induces a synergistic enhance in the bioavailability and antioxidant activity of polyphenolic compounds [14]. Kim et al., [15] also reported that paclitaxel and curcumin encapsulated in albumin NPs showing potential antitumor efficiency to pancreatic tumor cells.

Human serum albumin (HSA) is a natural carrier protein with a molecular weight of ~66 kDa and a high-affinity ligand-binding site [16-18]. HSA has been receiving great potential as an efficient bioactive and multifunctional biomolecule [19-23]. HSA as a carrier is biocompatible and biodegradable and has a number of chemical moieties for attachment to small molecules or ligands with different functional groups such as amines, hydroxyl, and carboxylates [24-27]. HSA in medicinal field can extend the circulating half-lives of small molecules like polyphenols as well

as be used as a nanoformulation system to enhance the function of ligands [28-30]. These positive points have extended the application of HSA in pharmaceutical and medical implementations.

Silymarin is the bioactive constituent of *Silybum marianum* L. (Milk thistle) which shows several effects such as anti-inflammatory/anti-fibrotic [31], hepatoprotective [32], anti-angiogenic [33], protective against cardiotoxicity [34], alleviative of Parkinson's associated pathologies [35], anti-viral [36], and antidiabetics [37]. It has been also documented that silymarin shows antioxidant features by scavenging free radicals and enhancing the glutathione levels, so that it can be used as a potential antioxidant agent and treatment of ischemia and reperfusion [38], liver damage [39], CNS disorders [40], cancer [41, 42], and cardiovascular diseases [43]. The particles of silymarin with poor solubility and low surface area may cause a poor absorption pursued to reduced bioactivity in higher dose of drug.

Therefore, it seems nanoformulation of silymarin by means of HSA may increase its solubility and antioxidant bioactivity. In this study we will explore the characterization of fabricated silymarin-HSA nanoplex. Afterwards, the antioxidant potential of prepared nanoplex will be compared to free silymarin in LPS-induced oxidative stress of nervous system *in vivo* and *in vitro.*

2. Materials and methods

2.1. Materials

HSA, Silymrin, Dulbecco's Modified Eagle's Medium with a 1:1 mixture of Hams F12 (DMEM:F12) and heat inactivated fetal bovine serum (FBS) were purchased from Sigma Co. (USA). All other materials were of analytical grade.

2.2. Methods

2.2.1. Preparation of silymarin-HSA nanoplex

The fabrication of silymarin-HSA nanoplex was carried out based on modified Yu Yu, Nguyen, Cheow and Hadinoto [44] method. Silymarin with *pKa* in the range of 6.63-7.95 was suspended in KOH (pH 13, 100 mN) at 5 mg/mL to form negatively charged silymarin solution. HSA with pI of 4.7 was dissolved in aqueous acetic acid solution [pH 2.95, 0.4% (v/v)] at 5 mg/mL to form HSA solution with positive charges distribution. Afterwards, equal volumes of the silymarin was added immediately dropwise into the HSA solutions with a stirring rate of 300 rpm. The resultant silymarin-HSA nanoplex solution was then centrifuged at 14,000 rpm at 4°C for 40 min and the pellet was re-suspended in deionized water.

2.2.2. Determination of encapsulation efficiency by HPLC

Silymarin was separated from the silymarin-HSA nanoplex by centrifugation of 14,000 rpm for 40 min. The concentration of free silymarin in the separated supernatant was then calculated by high performance liquid chromatography (HPLC, Agilent Technologies 1200 Infinity series, USA). The HPLC system consisted of a manual injector (20 µL sample loop) and UV-vis variable wavelength detector with an ultra C18, 5µm (250 × 4.6 mm, Restek, USA) with detection at 288 nm. Data was processed by Agilent HPLC Chemstation (Rev B.04.03).

Encapsulation efficiency was then determined using the following equations:

$$\text{Encapsulation efficiency}=W_{total}\text{-}W_{free}/W_{total}\times 100 \quad \text{Eq. 1}$$

2.2.3. Diameter and surface morphology

The samples were sonicated for 20 min by a sonicator probe (Misonix- S3000, USA) at room temperature with initial sonication power of 5 W. Afterwards, the sample were dropped on grid and dried at room temperature. The diameter and morphology of silymarin-HSA nanoplex were then determined by transmission electron microcopy (TEM, Zeiss - EM10C - 100 KV, Germany) and scanning electron micrograph (SEM, TESCAN vega3, Czech Republic), respectively.

2.2.4. Measurement of hydrodynamic radius and zeta potential

Hydrodynamic radius distribution and zeta potential of silymarin-HSA nanoplex were measured by dynamic light scattering (DLS, Zetasizer, Malvern, United Kingdom). The silymarin-HSA nanoplex samples were diluted with distilled water with a defined ratio and DLS experiment was carried out at room temperature. Every experiment was done for three times.

2.2.5. Fourier transform infrared spectroscopy (FTIR) Analysis

The presence of silymarin in the silymarin-HSA nanoplex was examined by FTIR spectroscopy (Perkin-Elmer, USA) at room temperature. The FTIR spectra in the dried state was evaluated between 400 and 4000 cm^{-1} with a spectral resolution of 1 cm^{-1} for the native silymarin, native HSA, silymarin-HSA nanoplex.

2.2.6. Molecular docking and dynamics studies

In order to optimize the geometry of silybin as a main component of silymarin molecule [45] the B3LYP functional [46, 47] (Lee et al., 2008) with the 3-21G basis set were employed. The optimization calculation was done using the Gaussian98W suite of program [48]. Molecular docking was executed using HEX 6.3 program [Ritchie et al., 2010]. The X-ray crystallographic 3D structure of HSA (PDB ID: 1AO6) was obtained from RCSB PDB (http://www.pdb.org).

In order to simulate the silybin/HSA interaction and formation of silybin-HSA nanoplex between the protein chains, the molecular dynamics simulation was performed using the LAMMPS [(Large-scale Atomic/Molecular Massively Parallel Simulator) code, (www.cs.sandia.gov/ wsjplimp/lammps.html), [49]] and Dreiding force field [50] as implemented in the software.

The molecular dynamics calculations were performed with two protein chains and one hundred charged silybin. The protein chains and silybin molecules were surrounded by water molecules and reached equilibrium temperatures of 298 K.

2.2.7. *In vitro* studies:

2.2.7.1. Cell culture

A human neuroblastoma cell line (SH-SY5Y) as a neuron-like cells was obtained from Royan institute for Stem Cell Biology and Technology (Tehran, Iran). The cells were cultured in a DMEM: F12 supplemented with 10% FBS, L-glutamine, penicillin, and streptomycin with concentrations of 2 mM, 100 IU/mL and 100 µg/mL, respectively. In all cellular assays, the SH-SY5Y cells were pre-treated with 10 µg/ml of silymarin or silymarin-HSA nanoplex for 24 h prior to the addition of LPS (20 µg/ml) [51]. Cells were then incubated for 24 h, and were eventually gone through cellular assays.

2.2.7.2. MTT assay

SH-SY5Y cells were cultured into a 96-well microplate at a density of 1×10^4 cells/well. After treatment, MTT assay was done to explore the cell viability. MTT solution with a concentration of 0.5 mg/ml was added for 4 h, the medium was gently removed, and the formed crystals were solubilized in DMSO. Absorbance of the sample was then read at 540 nm using an ELISA plate reader (Expert 96, Asys Hitch, Ec Austria). The negative control cells were considered as control cells and the relative viability was reported relative to the control cells.

2.2.7.3. Quantification of reactive oxygen species (ROS)

The formation of intracellular ROS was examined by an DCFDA / H_2DCFDA - Cellular ROS Assay Kit (ab113851) based on the manufacturer's protocol. Briefly, after treatment, cells were collected and incubated with DCFDA for 30 min. The fluorescence intensity was then analyzed by a FACS Calibur flow cytometry (BD Biosciences, San Jose, CA, USA).

2.2.7.4. Quantification of apoptosis

Quantification of apoptosis and necrosis was done based on the protocol provided by Annexin V-FITC Apoptosis Staining / Detection Kit (ab14085). Briefly, after treating, the cells were washed, trypsinized, and re-suspended in 500 µl of 1X Annexin V binding buffer. Afterwards, the cells were added by 5 µl of Annexin V-FITC and 5 µl propidium iodide followed by incubation at room temperature for 5 min in the dark. The amount of apoptosis and necrosis was then estimated using a FACS Calibur flow cytometry (BD Biosciences, San Jose, CA, USA).

2.2.8. *In vivo* studies

2.2.8.1. Animal handling

Male Wistar rats (200±250 g) were housed at 25°C and humidity of 55%, at 12 h light/dark cycle. Pellet food (Pharmacology department, Tehran University, Iran) and water were available ad libitum. The experiments were done based on the recommendations of the Iranian Code of Practice for the Care and Utilization of Animals for Scientific Thesis. The protocol was approved by the animal ethics committee of the Pharmacology Department, Tehran University, Iran

Thirty-two rats were divided randomly into four equal groups as follows: group I: control groups; group II: LPS; group III: LPS-induced oxidative stress pre-treated with silymarin; group (IV): LPS-induced oxidative stress pre-treated with silymarin-HSA nanoplex.

Rats were administrated by gavage at dose of 200 mg/kg silymarin or silymarin-HSA nanoplex over 3 days based on the Nencini, Giorgi and Micheli [52] study and at third day received LPS by IP at a dose of 0.5 mg/kg 150 min before scarification.

Rats were then killed by cervical dislocation and decapitation and the brains were immediately removed and kept at 80°C.

2.2.8.2. Brain homogenization and protein extraction

Samples (0.7 to 1.4 g of brain tissue) were homogenized in 5 volumes of pre-cooled isolation buffer [10 mM Tris–HCl (pH 7.4), 1 mM ethylenediaminetetraacetic acid (EDTA), 0.1% (w/v) bovine serum albumin (BSA), and 0.32 M sucrose] in a Teflon glass homogenizer. The homogenate was centrifuged at 13,500×g for 30 min, and the supernatant was collected and used for the measurement of superoxide dismutase (SOD) and catalase (CAT). Protein was determined according to the method of Bradford [53] using bovine serum albumin as standard.

2.2.8.3. Measurement of SOD and CAT activity

The activity of total SOD and CAT was measured by the method of Genet, Kale and Baquer [54] with some modification.

2.2.9. Statistical analysis

Statistical analyses were performed using SPSS software (SPSS Inc, Chicago, IL). Data were reported as mean ± SD. Statistical difference were determined using Student's t-test or one-way analysis of variance (ANOVA), considering $P < 0.05$ as statistically significant.

3. Results

3.1. Silymarin-HSA nanoplex characterization

Characterization of synthesized silymarin-HSA nanoplex was done by several techniques. TEM investigation showed that prepared silymarin-HSA nanoplex has a spherical shape with an average diameter between 50 nm to 150 nm (Fig. 1A). Also, it can be observed that HSA proteins formed a shell around silymarin molecules. SEM images also revealed the spherical shape of formed silymarin-HSA nanoplex with average size between 66 nm to 138 nm (Fig. 1B). DLS data displayed that the hydrodynamic radius of silymarin-HSA nanoplex is 188.3 nm with a PDI of 0.242 (Fig. 1C). Zeta potential analysis depicted that the charge distribution of prepared silymarin-

HSA nanoplex is around -26.6 mV (Fig. 1D), indicating an excellent colloidal stability of synthesized nanoplex. Analysis of the loading capacity of silymarin on HSA by HPLC reduces the testing time and the destruction of the HSA+silymarin combination in comparison to conventional methods which can releases silymarin from HSA at inappropriate time. Fig. 1 shows indicative chromatograms of HSA (Fig. 1E) and silymarin (Fig. 1F) standard solutions and silymarin-loaded HSA nanoplex solution (Fig. 1G). As can be observed in this Fig 1E, the relatively HSA peak has a retention time between 4.20 to 4.77 min approximately in standard HSA, and HSA+silymarin combination (Fig 1G). No peaks from devastation products based on HSA+silymarin combination observed in the chromatogram (Fig 1G). According to the area under curve (AUC), the increase in the diagram of silymarin from 1025.0 mAU*min to 997.3 mAU*min in HSA+silymarin combination, is indicative of the loading capacity of silymarin in HSA is approximately 97.3% based on equation 1.

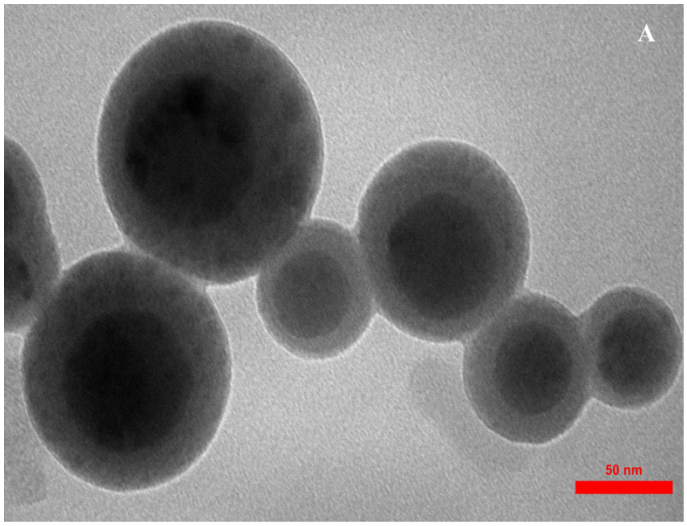

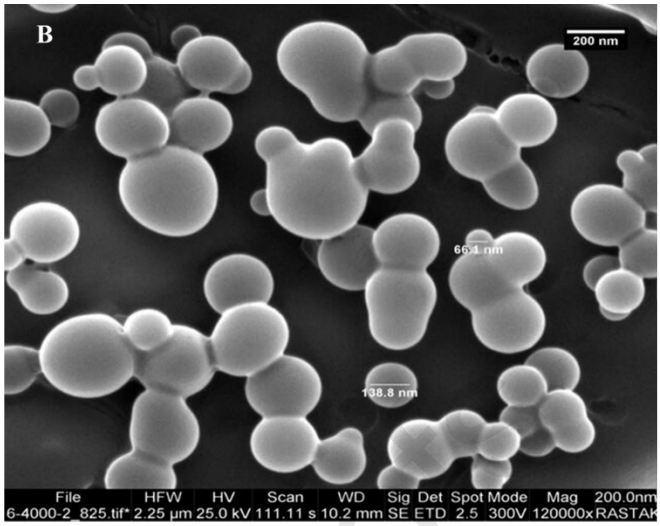

C

		Size (d.n...	% Intensity	Width (d.n...
Z-Average (d.nm): 188.3	Peak 1:	200.8	92.0	85.98
PdI: 0.242	Peak 2:	3463	8.0	1213
Intercept: 0.938	Peak 3:	0.000	0.0	0.000

Result quality Good

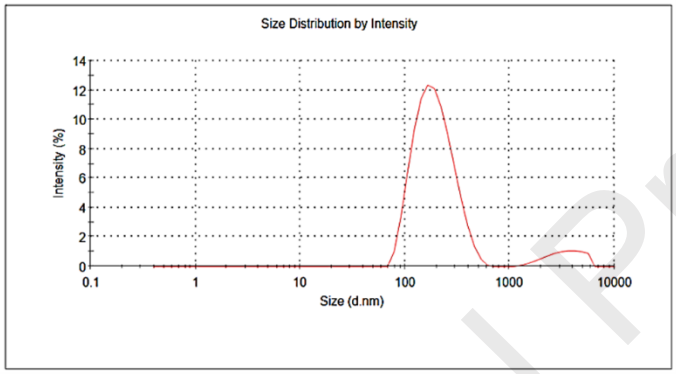

D

		Mean (mV)	Area (%)	Width (mV)
Zeta Potential (mV): -26.6	Peak 1:	-26.6	100.0	6.87
Zeta Deviation (mV): 6.87	Peak 2:	0.00	0.0	0.00
Conductivity (mS/cm): 0.318	Peak 3:	0.00	0.0	0.00

Result quality Good

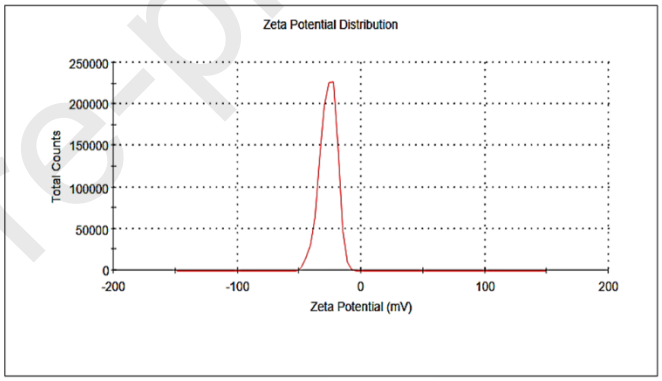

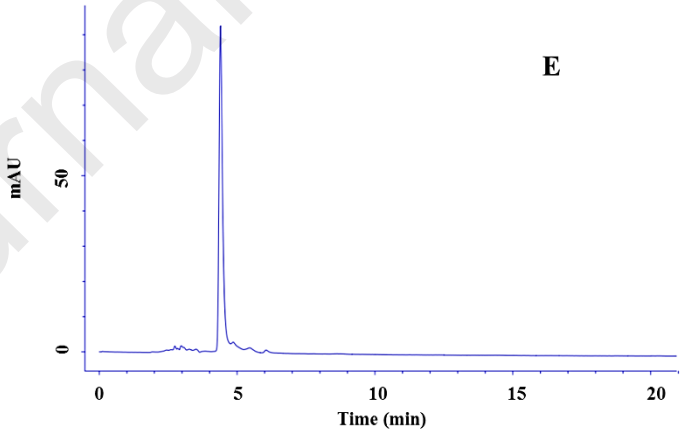

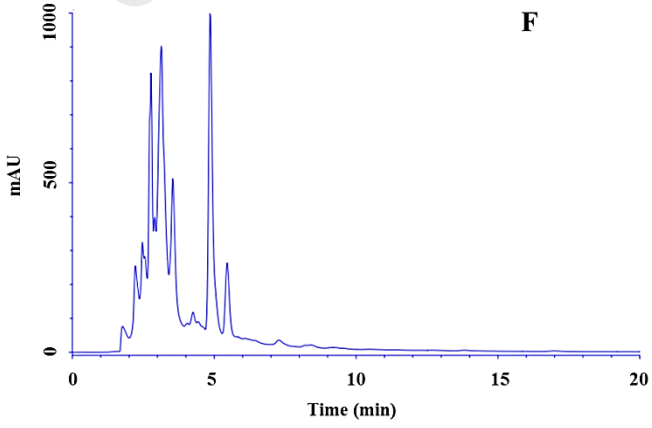

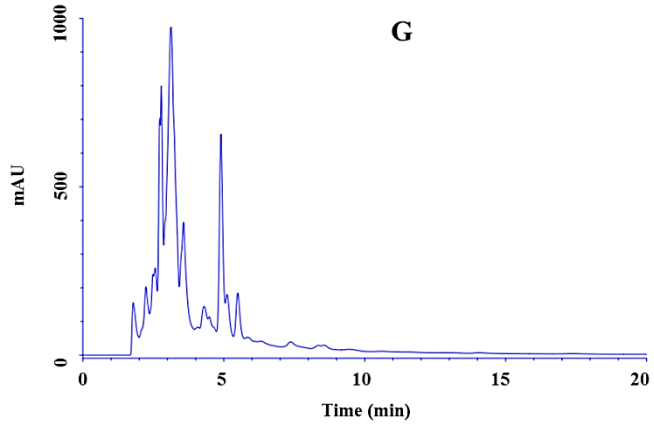

Figure 1. TEM (A), SEM (B), hydrodynamic radius (C), and zeta potential (D) investigations of prepared silymarin-HSA nanoplex. HSA chromatogram (E), silymarin chromatogram (F), and HSA-silymarin nanoplex chromatogram (G).

3.2. FTIR study

FTIR spectroscopy studies were carried out to reveal the silymarin and HSA interactions, the probable structural changes of HSA and presence of silymarin and HSA in the nanoformulation. The FT-IR spectra of silymarin (Fig. 2A), HSA (Fig. 2B) and silymarin-HSA nanoplex (Fig. 2C) are shown in Fig. 2. Fig. 2A shows spectrum of silymarin peak at 1645 cm^{-1} which is corresponded to stretching vibration of -C=C- alkenes and absorption signal at 1528 cm^{-1} is assigned to stretching vibration of C-C bonds of aromatic ring [55]. Fig. 2B depicts the FTIR spectrum of HSA which determines the presence of amide I and amide II peaks at 1668 cm−1 and 1548 cm−1, respectively [56]. Fig. 2C displays that the main FTIR peaks of silymarin and HSA were existed in the band of silymarin-HSA nanoplex and no significant shift was also observed especially for HSA molecules, suggesting the silymarin molecules loaded into HSA nanoplex and the structure of HSA was not significantly altered. Furthermore, no substantial shifted in the main bands of silymarin and HSA may suggest that no detectable bond was established between silymarin and albumin and silyamrim was entrapped into the HSA shell, which is in good agreement with TEM image.

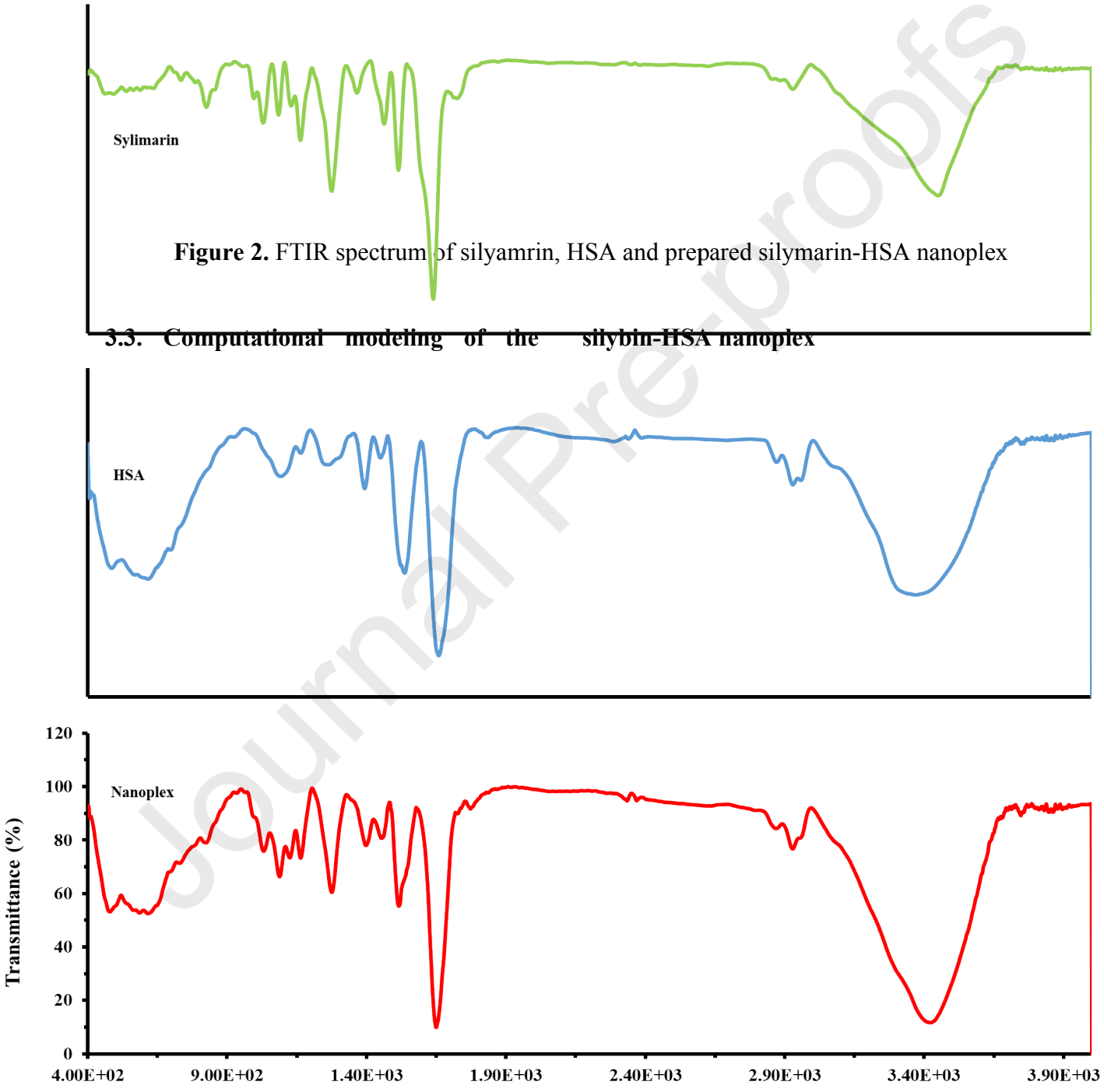

Figure 2. FTIR spectrum of silyamrin, HSA and prepared silymarin-HSA nanoplex

3.3. Computational modeling of the silybin-HSA nanoplex

In order to explore the potency of a small molecule as a biomedical drug, it is crucial to investigate the binding residues of that small molecule in biomolecules.

The optimized geometry of the silybin is shown in Fig. 3A. The molecular docking was performed with optimized structure of silybin (Fig. 3B). The E-value was found to be -371.90. Visualization of the binding site was performed by utilizing CHIMERA (www.cgl.ucsf.edu/chimera) and PyMOL (http://pymol.sourceforge.net/) programs. The contacting residues between silybin and HSA which are within 4 Å are LYS-444, CYS-448, TYR-457, ARG-218, ASP-340, PRO-339, ASN-295, GLU-294, TRP-214, and ASP-451 (Fig. 3C, D). There are 10 surrounding amino acids, five charged; three nonpolar; two polar.

It may be concluded that after interaction of silybin with HSA and encapsulation of silybin, several electrostatic, hydrophobic and hydrogenic interactions occur between silybin and HSA.

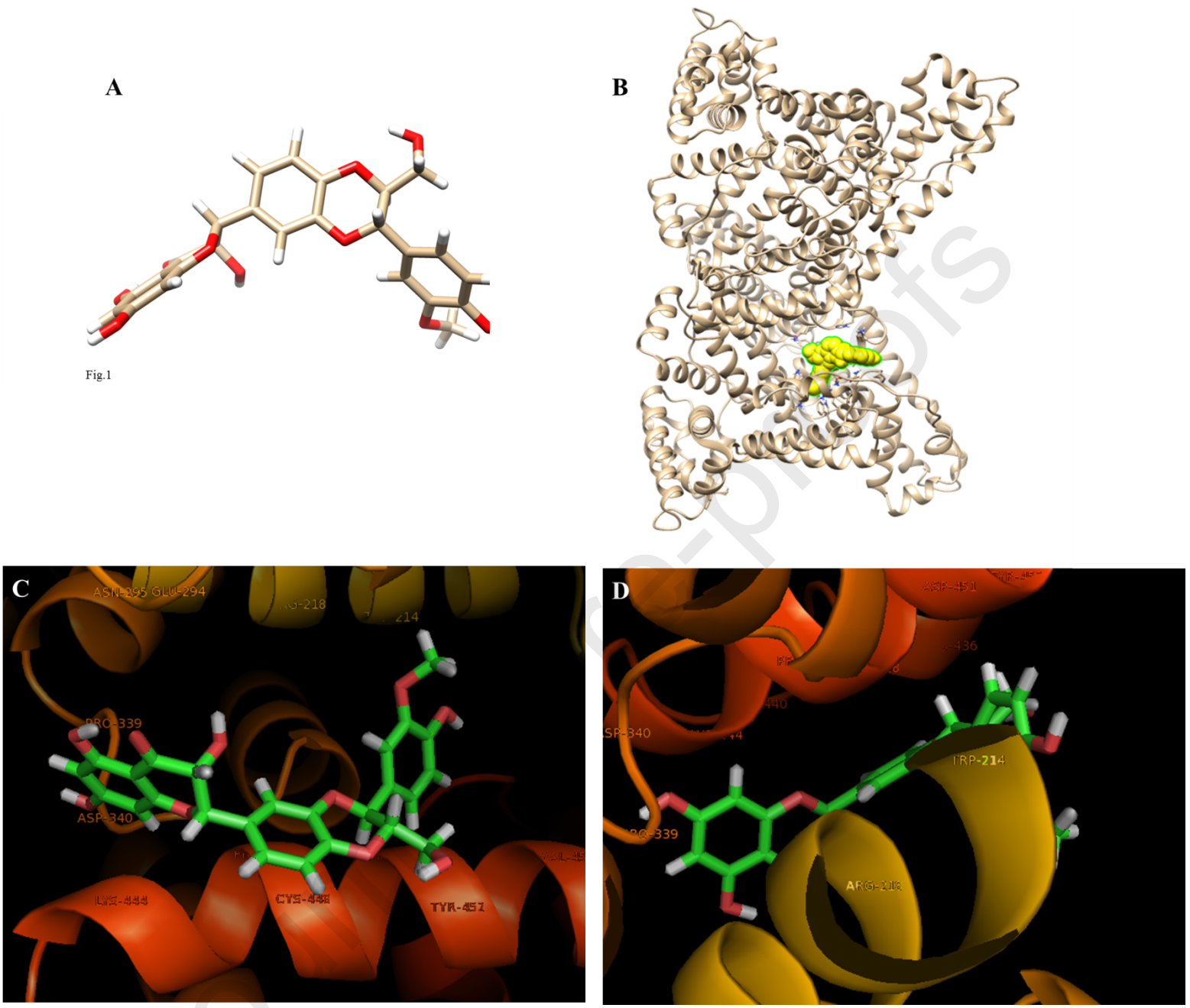

Fig.1

Figure 3. The optimized structure of the silybin (A), molecular docking outcome (B), Visualization of the binding site in two rotational views (C, D)

The NVE ensemble (time step of 1 fs, total simulation time of 100 ps) were employed in the modeling study. Visualization of the structures was done by using VMD tool (Humphrey et al., 1996).

Fig.4 shows the silybin -HSA nanoplex before and after the evolution. As can be observed, adsorbed silybin molecules which located between two protein chains tend to aggregate and construct the nanoplex. The rest of the silybin molecules enter the solvent. This data also is in good agreement with TEM and FTIR image, indicating the encapsulation of silymarin molecules into the HSA as a shell.

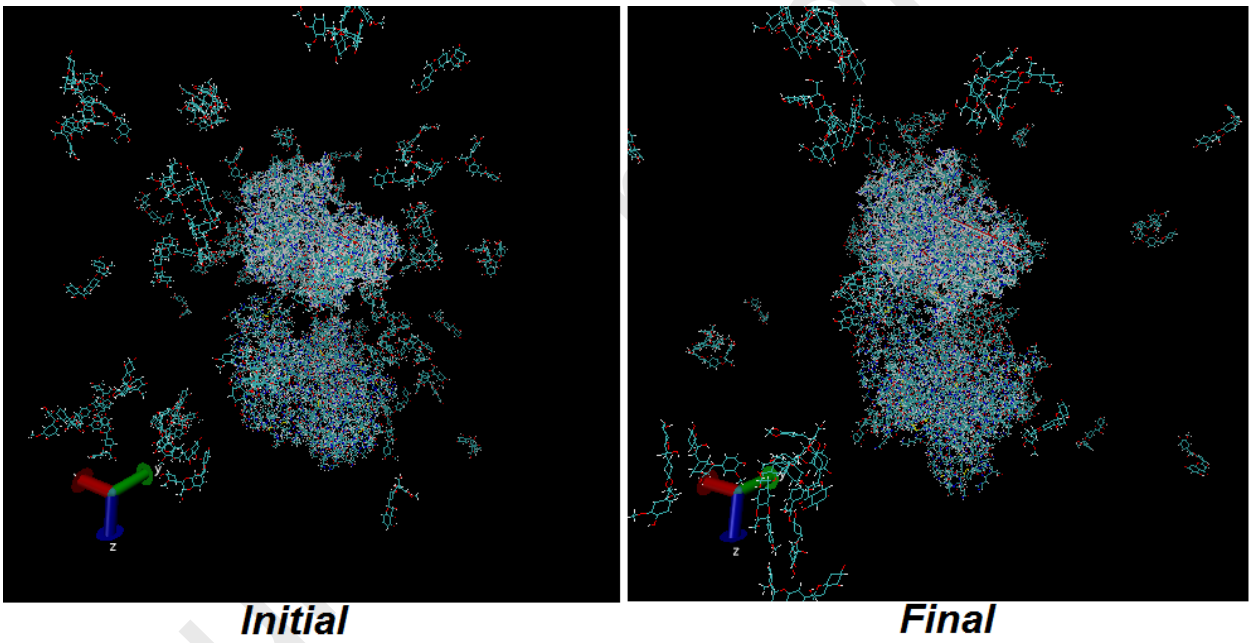

Figure 4. Silymarin-HSA nanoplex before and after the molecular dynamic evolution

3.4. In vitro assays

3.4.1. MTT assay

We found that silymarin and silymarin-HSA nanoplex till 10 µg/ml for 24 h and 48 h did not induce a significant toxicity against SH-SY5Y cells (data not shown). Therefore, this concentration was used as a safe dose to be used for protective effect of silymarin and nanosilymarin against LPS-induced cytotoxicity. MTT assay was performed to evaluate the protective effect of silymarin or silymarin-HSA nanoplex on cytotoxicity induced by LPS. It was shown that LPS with a concentration of 20 µg/ml causes a significant reduction in cell viability relative to control group (***P-value<0.001, relative to control group) (Fig. 5). However, pretreatment of cells with silymarin (10µg/ml) or silymarin-HSA nanoplex (10µg/ml) results in elevation of cell viability form 29.43±5.83% to 52.89±10.46% ($^{\#}$P-value<0.05, relative to LPS-treated group) and 7.74±3.03% ($^{\#\#}$P-value<0. 01, relative to LPS-treated group), respectively (Fig. 5). Also, it was determined that silymarin-HSA nanoplex protect the cells more significantly ($^{\&}$P-value<0. 01, relative to LPS-treated group pre-incubated with silymarin) than natural silymarin against LPS-stimulated cytotoxicity.

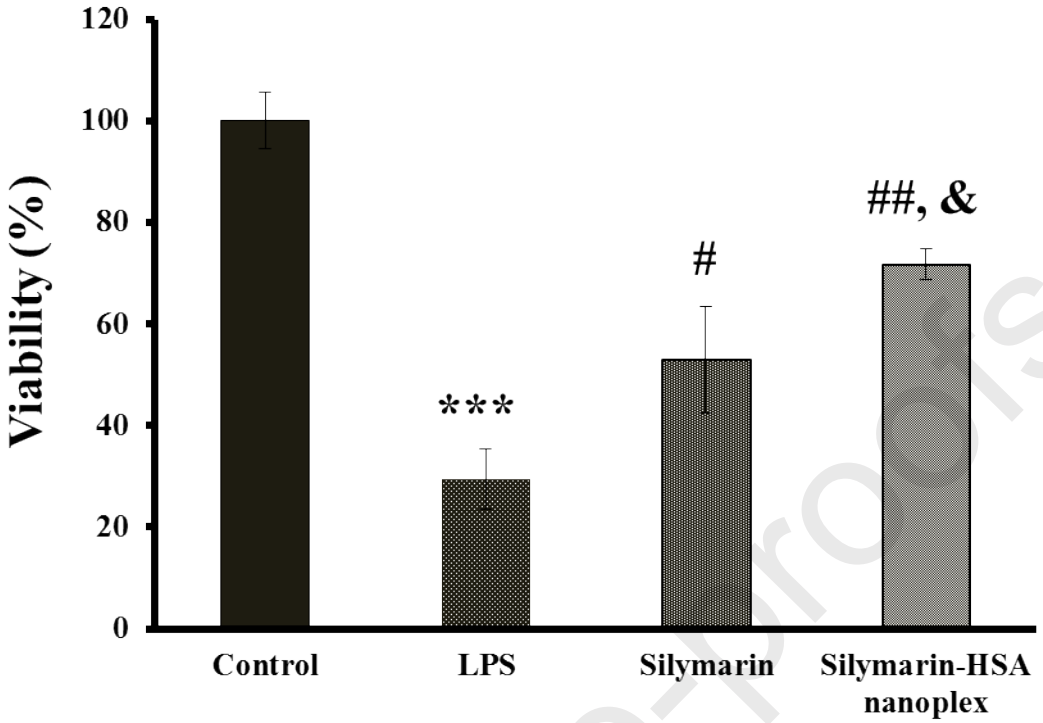

Figure 5. MTT assay of control group, LPS-treated group, LPS-treated group pre-treated with silymarin, and LPS-treated group pre-treated with silymarin-HSA nanoplex. After treating cells with either silymarin or silymarin-HSA nanoplex for 24 h, cells were then incubated with LPS for 24 h, and MTT assay was done.
***P-value<0.001, relative to control group, #P-value<0.05, relative to LPS-treated group, ##P-value<0. 01, relative to LPS-treated group, &P-value<0. 01, relative to LPS-treated group pre-incubated with silymarin

3.4.2. Reactive oxygen species (ROS) generation study

A flow cytometry investigation was done to speculate the protective effect of silymarin or silymarin-HSA nanoplex against LPS-triggered oxidative stress. As shown in Fig. 6, the mean DCFH fluorescence intensities of control group, LPS-treated group, LPS-treated group pre-treated with silymarin, and LPS-treated group pre-treated with silymarin-HSA nanoplex were 77.1 (Fig. 6A), 624 (Fig. 6B), 264(Fig. 6C), and 162 (Fig. 6D), respectively. As summarized in Table 1, it

can be dedicated that LPS significantly enhanced the production of intracellular ROS (***P-value<0.001, relative to control group), however pretreatment of cells with silymarin ($^{\#\#}$P-value<0.01, relative to LPS-treated group) or silymarin-HSA nanoplex ($^{\#\#\#}$P-value<0.001, relative to LPS-treated group) resulted in a significant reduction of ROS generation relative to LPS control group. Moreover, it was revealed that silymarin-HSA nanoplex reduced the production of ROS more significantly ($^{\&}$P-value<0.05, relative to LPS-treated group pre-treated with silymarin) than natural silymarin against LPS-stimulated oxidative stress.

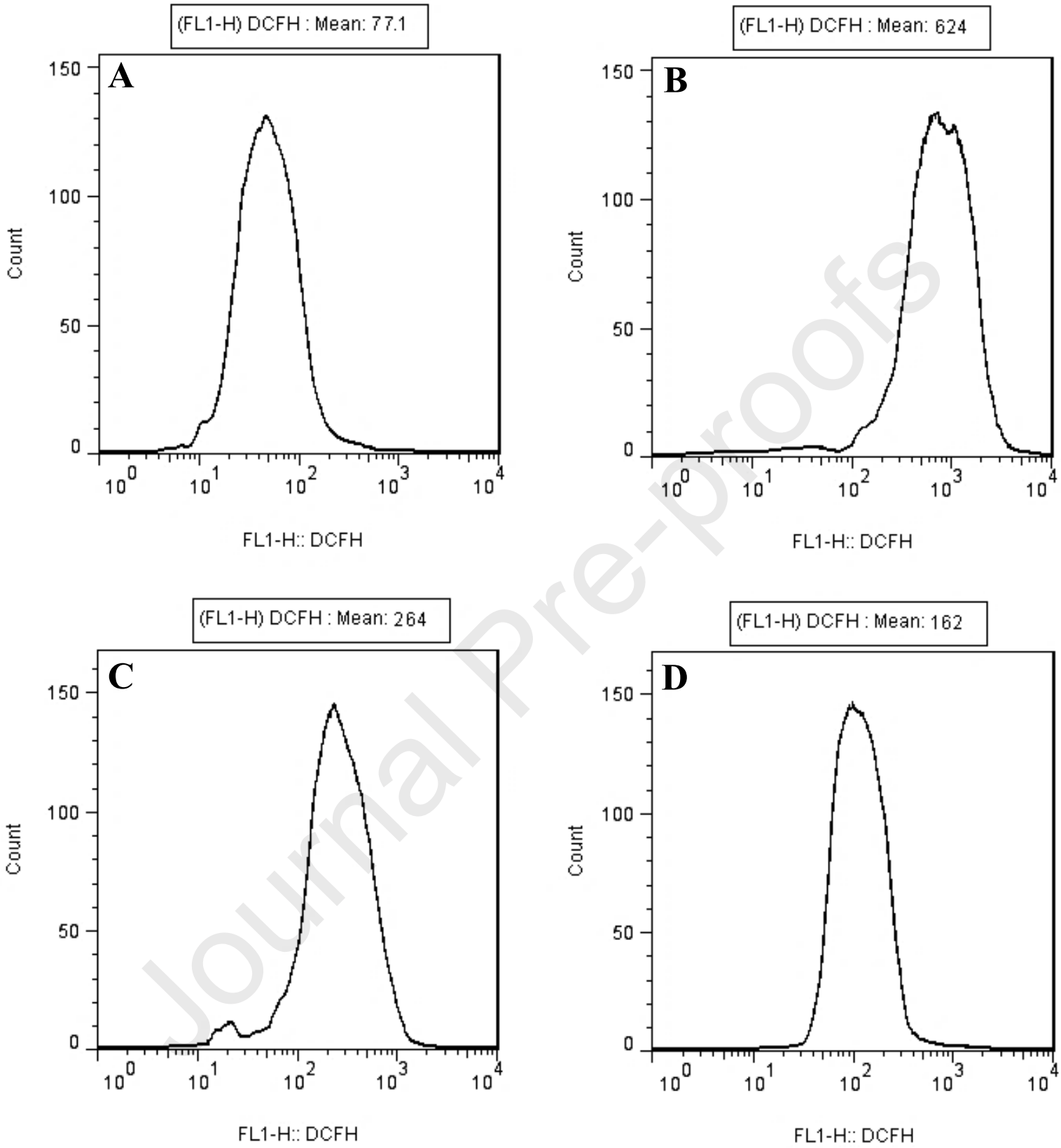

Figure 6. Flow cytometry analysis for quantification of ROS. Control cells (A), LPS-treated cells (B), LPS-treated cells pre-treated with silymarin (C), and LPS-treated cells pre-treated with silymarin-HSA nanoplex (D).

Table 1. Statistical analysis to compare the ROS generation between treated groups and negative control cells

Group	**ROS (units)**	**P-value**
control	77.1	-
LPS-treated group	624	***P-value<0.001, relative to control group
LPS-treated group pre-treated with silymarin,	264	##P-value<0.01, relative to LPS-treated group
LPS-treated group pre-treated with silymarin-HSA nanoplex	162	###P-value<0.001, relative to LPS-treated group, &P-value<0.05, relative to LPS-treated group pre-treated with silymarin,

3.4.3. Apoptosis analysis

To study whether the *in vitro* LPS-incubated SH-SY5Y cells encounter toxicity through the mechanism of apoptosis, quantification of apoptosis was determined using flow cytometry analysis. It was shown in Fig. 7 that the amount of early apoptosis (Q3), late apoptosis (Q2), and necrosis (Q1) significantly increases form 0.32%, 0.84% and 2.8% in control group (Fig .7A) to 8.81% (***P-value< 0.001, relative to control group) , 39.45% (***P-value< 0.001, relative to control group), and 30.54% (***P-value< 0.001, relative to control group) in LPS-treated group (Fig. 7B). However, pretreatment of cells with silymarin or silymarin-HSA nanoplex resulted in significant reduction of early apoptosis, late apoptosis and necrosis to 1.28% ($^{###}$P-value< 0.001, relative to LPS-treated group), 11.8% ($^{###}$P-value< 0.001, relative to LPS-treated group), 21.82% ($^{#}$P-value< 0.05, relative to LPS-treated group) (Fig. 7C) and 3.01% ($^{###}$P-value< 0.001, relative to LPS-treated group), 4.14% ($^{###}$P-value< 0.001, relative to LPS-treated group), 9.55% ($^{###}$P-value< 0.001, relative to LPS-treated group) (Fig. 7D), respectively.

Furthermore, it was demonstrated that silymarin-HSA nanoplex decreased the amount of late apoptosis ($^{\&\&}$P-value<0.01, relative to LPS-treated group pre-treated with silymarin) and necrosis more remarkably ($^{\&\&}$P-value<0.01, relative to LPS-treated group pre-treated with silymarin) than natural silymarin against LPS-stimulated oxidative stress.

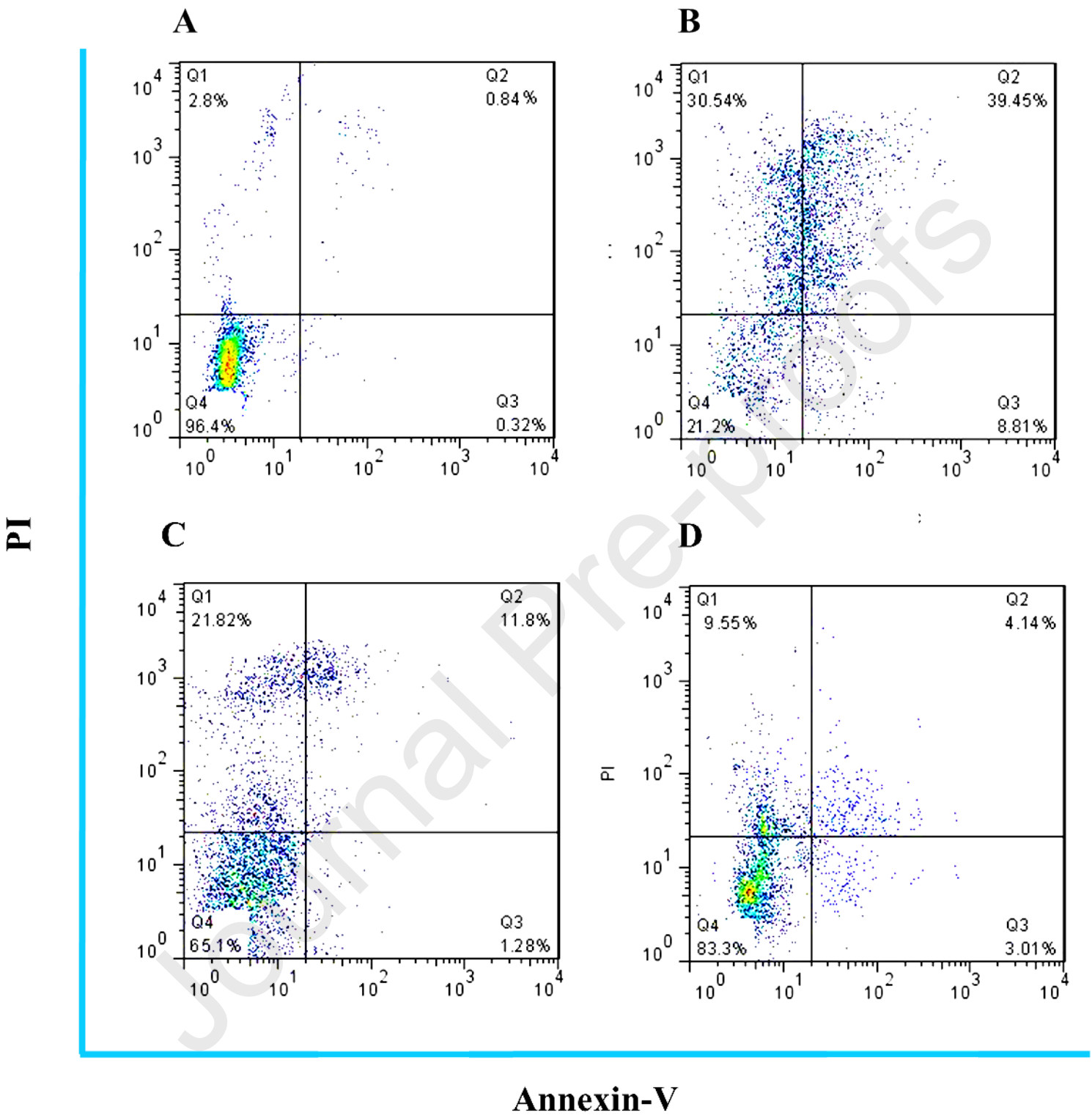

Figure 7. Flow cytometry analysis for quantification of apoptosis and necrosis. Control cells (A), LPS-treated cells (B), LPS-treated cells pre-treated with silymarin (C), and LPS-treated cells pre-treated with silymarin-HSA nanoplex (D).

3.5. In vivo assays

3.5.1. CAT and SOD activity assays

The activity of CAT and SOD in rat brains were assayed to reveal the protective effect of silymarin and silymarin-HSA nanoplex. As shown in Fig. 8A, the CAT activities in control group, LPS group, LPS group treated with silymarin, and LPS group treated with silymarin-HSA nanoplex were 3.60±0.31 unit/mg protein, 2.28±0.21 unit/mg protein (*P-value< 0.05, relative to control group), 2.57±0.20 unit/mg protein, and 9.22±1.85 unit/mg protein ($^{###}$P-value< 0.001, relative to LPS-treated group), respectively. Also, it was depicted that silymarin-HSA nanoplex increased the CAT activity more significantly ($^{\&\&\&}$P-value<0.001, relative to LPS-treated group pre-treated with silymarin) than natural silymarin against LPS-stimulated oxidative stress.

The SOD activities in control group, LPS group, LPS group treated with silymarin, and LPS group treated with silymarin-HSA nanoplex were also shown to be 89.71±4.62 unit/mg protein, 75.87±6.05 unit/mg protein (*P-value< 0.05, relative to control group), 91.56±9.36 unit/ mg protein ($^{\#}$P-value< 0.05, relative to LPS-treated group), and 109.19±18.44 unit/mg protein ($^{\#\#}$P-value< 0.01, relative to LPS-treated group), respectively (Fig. 8B). Furthermore, it was displayed that silymarin-HSA nanoplex increased the SOD activity more significantly ($^{\&}$P-value<0.05, relative to LPS-treated group pre-treated with silymarin) than natural silymarin against LPS-induced oxidative stress.

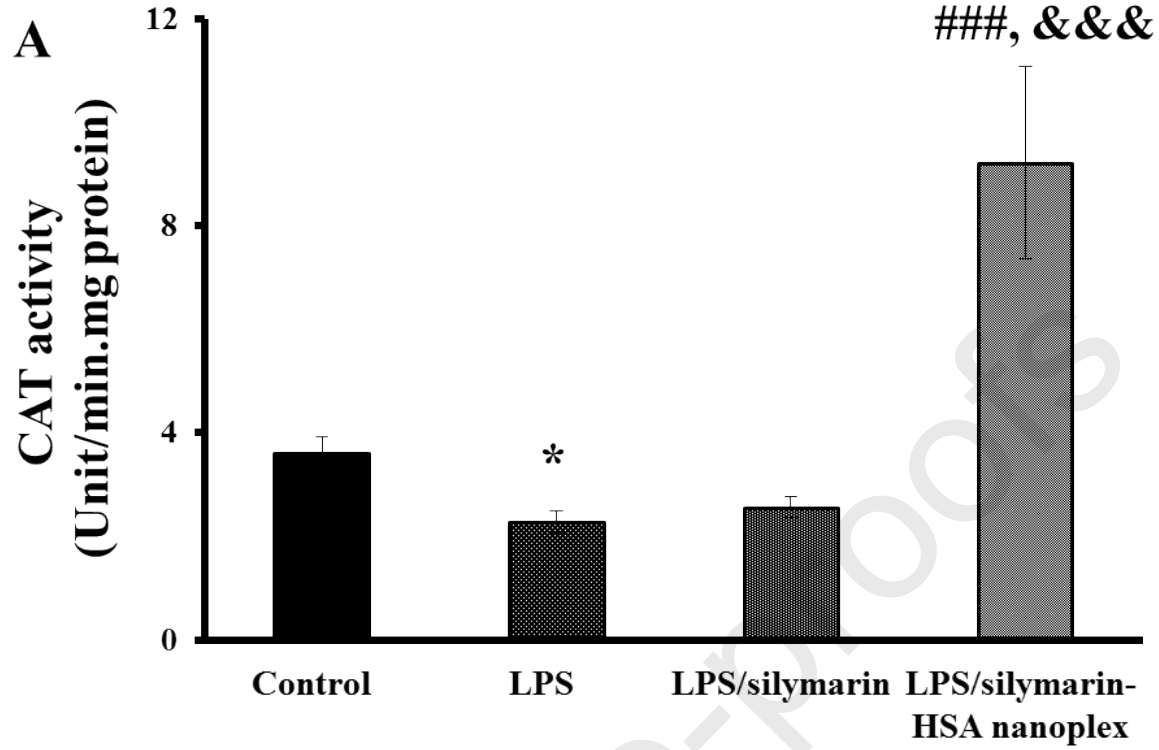

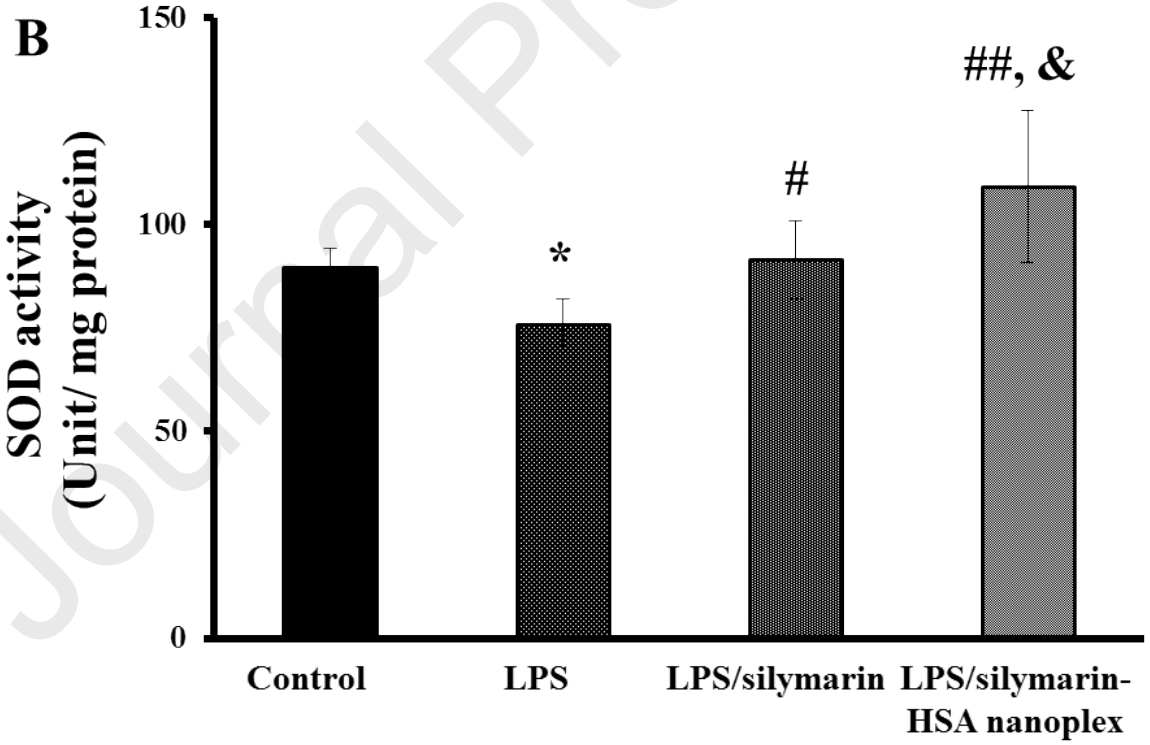

Figure 8. CAT (A) and SOD (B) activity assay in brain tissue of rats treated with LPS, LPS/silymarin or LPS/silymarin-HSA nanoplex.

*P-value< 0.05, relative to control group, ###P-value< 0.001, relative to LPS-treated group, &&&P-value<0.001, relative to LPS-treated group pre-treated with silymarin, #P-value< 0.05, relative to LPS-treated group, ##P-value< 0.01, relative to LPS-treated group, &P-value<0.05, relative to LPS-treated group pre-treated with silymarin.

4. Discussion

In this study prepared silymarin-HSA nanoplex was characterized by different techniques. Afterwards, the protective effect of synthesized silymarin-HSA nanoplex against LPS-induced cytotoxicity in SH-SY5Y cells was explored by MTT, ROS and apoptosis assays. In the next step, the protective impact of silymarin-HSA noncomplex against LPS-induced inactivation of SOD and CAT in brain tissue of rats was investigated. Our data presented that silymarin-HSA nanoplex was successfully fabricated and provide promising outcomes against LPS-induced toxicity *in vitro* and *in vivo*. Parallel to this result Fang Fang, Hao, Wu, Li, Leng and Jing [57] reported that quercetin shows promising antioxidant function, however, the poor stability hinders its application in biomedical systems. Therefore, they came to decision to fabricate a BSA- quercetin nanoplex. The outcomes indicated that the average size of fabricated nanoplex was less than 10 nm. Albumin NPs not only enhanced the stability of nano-quercetin, but also preserved the antioxidant function of entrapped compound [57]. They also showed that contributing interactions between BSA and quercetin were both hydrophobic and hydrophilic forces, which is in accordance with our data. They proposed that BSA could be a potential vehicle to fabricate the nanocomplex for efficient delivery of hydrophobic compounds to the targeted sites [57]. Soudi et al., [58] also revealed that nano-encapsulation of berberine can provide a protective effect against neuroprotective diseases. They explored the impact of modified berberine/chitosan nanoconjugate against LPS-stimulated neurodegenerative disorders and hepatotoxicity *in vivo*. The protective effects of nano-berberine

compared to free berberine were observed to be linked with the physicochemical properties of fabricated nanocomplex [58]. Rashidian et al., [59] also reported the the protective impact of nano-curcumin in acute pancreatitis through reduction of inflammatory responses. Fakhraei et al., [60] depicted that acute administration of nano-curcumin decreased the depression-like behaviors without affecting the general locomotor activity more efficiently then free curcumin. They concluded that the neuroprotective impact of nano-curcumin species is associated with their anti-inflammatory and free radical scavenging in the nervous system [60]. Shukla et al., [61] displayed that chitosan covered curcumin NPs ameliorate pharmacotherapy via increased pharmacokinetics and interplay of anti-inflammatory genes in Gram negative sepsis. Papay et al., [62] developed apigenin-BSA nanoplex and its application as a nanovehicle for selective treatment of pulmonary inflammation. They found that the encapsulation efficiency was around 82%. The antioxidant activity revealed that the free radical scavenging of apigenin-BSA nanoplex remind almost similar to the free counterparts [62]. Ghosh et al., [63] prepared fisetin-HSA nanoplex to increase its bioactivity. The fabricated nanoplex showed an average diameter of 220 nm with an encapsulation potency of 84%. The antioxidant function and anticancer activity of the fabricated nanoplex showed that this system can be utilized for the targeted drug deivery. Das et al., [64] showed that silymarin NPs synthesized based on a polymer with a size of around 120 nm could increase the glutathione level in hepatic tissue and play a protective effect against drug-stimulated hepatotoxicity. Yang etv al., [65] also depicted that silymarin-loaded liquid nanoemulsion could significantly reduce the hepatotoxicity more efficiently that commercial agents. Younis, Shaheen and Abdallah [66] manifested that silymarin- Eudragit® RS100 nanoplex reverse liver activity and fibrosis and mitigate oxidative stress and inflammation *in vivo* [66]. In general, Hsu et al., [67], Shangguan et al., [68], Guhagarkar et al., [69], Cengiz et al., [70], Ma et al., [71], Abdel-Wahhab

et al., [72], Liang et al., [73] and Ashraf et al., [74] showed that silymarin NPs can provide more efficient biomedical activity than free counterparts.

In general antioxidant activities of silymarin are based on three pathways, including elimination of free radicals directly [75, 76], preventing free radical generation by inhibiting the associated enzymes [77], and maintaining optimal redox state of the cell by activating a wide range of enzymatic and non-enzymatic antioxidants through transcription factors [78, 79]. In this regard, Zhao, Deng [80] by increasing the stability and solubility of silymarin particles via emulsion solvent evaporation and freeze-drying methods emulation, in addition to enhancing the bioavailability and absorption capability of silymarin in the intestine, improved the accumulation of silymarin in the liver and their hepatoprotective activities against free radicals. Likewise, Abdel-Wahhab, El-Nekeety [81] by using silymarin NPs, was able to significantly reduce liver injury by limiting the activity of free radicals derived from fusarium toxin (Deoxynivalenol) present in cereal diets. Recently, in a mice model, oral administration of silymarin NPs (200 mg/kg) showed that not only silymarin NPs had high antidepressant effects compared to fluoxetine, it reduced oxidative stress and neuronal inflammation induced by oxidant in the cerebral cortex and hippocampus along with increasing levels of neurotransmitters [82].

In this study, it seems HSA-silymarin nanoplex mitigates the LPS-induced oxidative stress by an increase in the activity of antioxidant enzymes such as CAT and SOD.

As a number of diseases are associated with the elevation ROS, therefore reducing the ROS level could be considered as key issue in treatment and inhibition of several disorders such as neurodegenerative, liver and cardiovascular diseases. Silymarin as a potent antioxidant compound may be used as a promising candidate in prevention of a wide number of disorders. However, it shows low bioavailability due to its strong hydrophobic characteristics and high membrane and

blood brain barrier impermeability. Unfortunately, few reports have addressed the fabrication of proper oral nanovehicles that can potentially deliver flavonoids like silymarin to the targeted tissues and increase its antioxidant effects. Therefore, silymarin-HSA nanoplex was fabricated in this paper and evaluated their ROS-lowering impact *in vitro* and *in vivo* in LPS-mediated models. In the future studies, the profile of silymarin release in different pHs by analytical HPLC and the mechanism of antioxidant properties of silymarin-HSA nanoplex could be investigated to may open new avenues to design and develop potential nanosilymarin compounds for therapeutic systems.

5. Conclusion

Silymarin-HSA nanoplex was prepared by encapsulation of silymarin in HSA matrix. Antioxidant and antiapoptotic activity of silymarin-HSA nanoplex were increased more significantly than free counterparts against LPS-induced toxicity in neuron like cells and brain tissue. The present study may furnish details to reveal that albumin-nanoplex is potential vehicles of silymarin and the application of traditional or unique excipients should be beard into mind. Indeed, the developed silymarin-HSA nanoplex can be utilized as a novel delivery carrier against neurodegenerative disorders with prospective antioxidant activity.

Acknowledgment

The research has been supported by Tehran University of Medical Sciences & Health Services grant NO. 97023038702, Tehran, Iran.

Conflict of interest

The authors declare no conflict of interest

References:

[1] B. Hu, X. Liu, C. Zhang, X. Zeng, Food macromolecule based nanodelivery systems for enhancing the bioavailability of polyphenols, J. Food Drug Anal. 25(1) (2017) 3-15.
[2] J. Liang, H. Yan, P. Puligundla, X. Gao, Y. Zhou, X. Wan, Applications of chitosan nanoparticles to enhance absorption and bioavailability of tea polyphenols: A review, Food Hydrocolloids 69 (2017) 286-292.
[3] S. Pimentel-Moral, M.C. Teixeira, A.R. Fernandes, D. Arraez-Roman, A. Martinez-Ferez, A. Segura-Carretero, E.B. Souto, Lipid nanocarriers for the loading of polyphenols - A comprehensive review, Adv. Colloid Interface Sci. 260 (2018) 85-94.
[4] A. Celebioglu, Z.I. Yildiz, T. Uyar, Thymol/cyclodextrin inclusion complex nanofibrous webs: Enhanced water solubility, high thermal stability and antioxidant property of thymol, Food Res. Int. 106 (2018) 280-290.
[5] Z. Li, H. Jiang, C. Xu, L. Gu, A review: Using nanoparticles to enhance absorption and bioavailability of phenolic phytochemicals, Food Hydrocolloids 43 (2015) 153-164.
[6] S. Manju, K. Sreenivasan, Conjugation of curcumin onto hyaluronic acid enhances its aqueous solubility and stability, J. Colloid Interface Sci. 359(1) (2011) 318-325.
[7] Y.M. Tsai, C.F. Chien, L.C. Lin, T.H. Tsai, Curcumin and its nano-formulation: the kinetics of tissue distribution and blood-brain barrier penetration, Int. J. Pharm. 416(1) (2011) 331-8.
[8] A.F. Esfanjani, S.M. Jafari, Biopolymer nano-particles and natural nano-carriers for nano-encapsulation of phenolic compounds, Colloids Surf. B. Biointerfaces 146 (2016) 532-543.
[9] C. Guo, J. Yin, D. Chen, Co-encapsulation of curcumin and resveratrol into novel nutraceutical hyalurosomes nano-food delivery system based on oligo-hyaluronic acid-curcumin polymer, Carbohydr. Polym. 181 (2018) 1033-1037.
[10] Y. Ding, L. Zou, C. Lu, H. Tong, B. Chen, In situ enzymatic synthesis and purification of theaflavin-3, 3'-digallate monomer and incorporation into nanoliposome, Int. J. Food Sci. Technol. 53(11) (2018) 2552-2559.
[11] V. Van Tran, J.-Y. Moon, Y.-C. Lee, Liposomes for delivery of antioxidants in cosmeceuticals: Challenges and development strategies, J. Control. Release (2019).
[12] Y. Fan, Y. Liu, L. Gao, Y. Zhang, J. Yi, Improved chemical stability and cellular antioxidant activity of resveratrol in zein nanoparticle with bovine serum albumin-caffeic acid conjugate, Food Chem. 261 (2018) 283-291.
[13] W. Xu, P. Ge, L. Huang, Z. Du, X. Liu, J. Li, N. Yang, Solubilization and protection of curcumin based on lysozyme/albumin nano-complex, AIP Advances 8(11) (2018) 115221.
[14] M. Bonoli-Carbognin, L. Cerretani, A. Bendini, M.P. Almajano, M.H. Gordon, Bovine serum albumin produces a synergistic increase in the antioxidant activity of virgin olive oil phenolic compounds in oil-in-water emulsions, J. Agric. Food Chem. 56(16) (2008) 7076-7081.
[15] B. Kim, C. Lee, E.S. Lee, B.S. Shin, Y.S. Youn, Paclitaxel and curcumin co-bound albumin nanoparticles having antitumor potential to pancreatic cancer, asian journal of pharmaceutical sciences 11(6) (2016) 708-714.
[16] Y. Gou, Y. Zhang, F. Yang, H. Liang, Evaluation of interactions between platinum-/ruthenium-based anticancer agents and human serum albumin: development of HSA carrier for metal-based drugs, Curr. Pharm. Des. 21(14) (2015) 1848-1861.
[17] U. Bairagi, P. Mittal, B. Mishra, Albumin: a versatile drug carrier, Austin Therapeutics 2(2) (2015) 1021.
[18] P. Lee, X. Wu, Modifications of human serum albumin and their binding effect, Curr. Pharm. Des. 21(14) (2015) 1862-1865.
[19] U. Kragh-Hansen, Human serum albumin: a multifunctional protein, Albumin in Medicine, Springer2016, pp. 1-24.
[20] F.-F. An, X.-H. Zhang, Strategies for preparing albumin-based nanoparticles for multifunctional bioimaging and drug delivery, Theranostics 7(15) (2017) 3667.

[21] C. Li, X. Wang, H. Song, S. Deng, W. Li, J. Li, S. Jin, Current multifunctional albumin-based nanoplatforms for cancer multi-mode therapy, Asian Journal of Pharmaceutical Sciences (2019).
[22] J.P. Martins, R. D'Auria, D. Liu, F. Fontana, M.P. Ferreira, A. Correia, M. Kemell, K. Moslova, E. Mäkilä, J. Salonen, Engineered Multifunctional Albumin-Decorated Porous Silicon Nanoparticles for FcRn Translocation of Insulin, Small 14(27) (2018) 1800462.
[23] A. Sahu, J.H. Lee, H.G. Lee, Y.Y. Jeong, G. Tae, Prussian blue/serum albumin/indocyanine green as a multifunctional nanotheranostic agent for bimodal imaging guided laser mediated combinatorial phototherapy, J. Control. Release 236 (2016) 90-9.
[24] A. Nezami, S. Dehghani, R. Nosrati, N. Eskandari, S.M. Taghdisi, G. Karimi, Nanomaterial-based biosensors and immunosensors for quantitative determination of cardiac troponins, J. Pharm. Biomed. Anal. 159 (2018) 425-436.
[25] M.W. Sabaa, D.H. Hanna, M.H. Abu Elella, R.R. Mohamed, Encapsulation of bovine serum albumin within novel xanthan gum based hydrogel for protein delivery, Mater. Sci. Eng. C Mater. Biol. Appl. 94 (2019) 1044-1055.
[26] C. Tao, Y.J. Chuah, C. Xu, D.-A. Wang, Albumin conjugates and assemblies as versatile bio-functional additives and carriers for biomedical applications, Journal of Materials Chemistry B 7(3) (2019) 357-367.
[27] A. Upadhyay, R. Kandi, C.P. Rao, Injectable, self-healing, and stress sustainable hydrogel of BSA as a functional biocompatible material for controlled drug delivery in cancer cells, ACS Sustainable Chemistry & Engineering 6(3) (2018) 3321-3330.
[28] J. Feng, C. Zhao, L. Wang, L. Qu, H. Zhu, Z. Yang, G. An, H. Tian, C. Shou, Development of a novel albumin-based and maleimidopropionic acid-conjugated peptide with prolonged half-life and increased in vivo anti-tumor efficacy, Theranostics 8(8) (2018) 2094.
[29] M.T. Larsen, H. Rawsthorne, K.K. Schelde, F. Dagnæs-Hansen, J. Cameron, K.A. Howard, Cellular recycling-driven in vivo half-life extension using recombinant albumin fusions tuned for neonatal Fc receptor (FcRn) engagement, J. Control. Release 287 (2018) 132-141.
[30] C. Wang, C. Zhang, Z. Li, S. Yin, Q. Wang, F. Guo, Y. Zhang, R. Yu, Y. Liu, Z. Su, Extending Half Life of H-Ferritin Nanoparticle by Fusing Albumin Binding Domain for Doxorubicin Encapsulation, Biomacromolecules 19(3) (2018) 773-781.
[31] N.M. El-Lakkany, O.A. Hammam, W.H. El-Maadawy, A.A. Badawy, A.A. Ain-Shoka, F.A. Ebeid, Anti-inflammatory/anti-fibrotic effects of the hepatoprotective silymarin and the schistosomicide praziquantel against Schistosoma mansoni-induced liver fibrosis, Parasites & vectors 5(1) (2012) 9.
[32] M. Saeed, D. Babazadeh, M. Arif, M.A. Arain, Z.A. Bhutto, A.H. Shar, M.U. Kakar, R. Manzoor, S. Chao, Silymarin: a potent hepatoprotective agent in poultry industry, Worlds Poult. Sci. J. 73(3) (2017) 483-492.
[33] S.-H. Yang, J.-K. Lin, W.-S. Chen, J.-H. Chiu, Anti-angiogenic effect of silymarin on colon cancer LoVo cell line, J. Surg. Res. 113(1) (2003) 133-138.
[34] B.M. Razavi, G. Karimi, Protective effect of silymarin against chemical-induced cardiotoxicity, Iran J Basic Med Sci 19(9) (2016) 916-923.
[35] S. Srivastava, S.R. Sammi, T.S. Laxman, A. Pant, A. Nagar, S. Trivedi, R.S. Bhatta, S. Tandon, R. Pandey, Silymarin promotes longevity and alleviates Parkinson's associated pathologies in Caenorhabditis elegans, J. Funct. Foods 31 (2017) 32-43.
[36] A. Castellaneta, A. Massaro, M. Rendina, F. D'Errico, S. Carparelli, S.F. Rizzi, A.W. Thomson, A. Di Leo, Immunomodulating effects of the anti-viral agent Silibinin in liver transplant patients with HCV recurrence, Transplantation research 5 (2016) 1-1.
[37] A.L. Chan, H.W. Leung, T.-W. Chien, S.-J. Lin, Pattern of co-prescription of silymarin and antidiabetics in outpatient, a population based study, Journal of Medicinal Food Plants 1(2) (2009).
[38] F. Turgut, O. Bayrak, F. Catal, R. Bayrak, A.F. Atmaca, A. Koc, A. Akbas, A. Akcay, D. Unal, Antioxidant and protective effects of silymarin on ischemia and reperfusion injury in the kidney tissues of rats, Int. Urol. Nephrol. 40(2) (2008) 453-460.

[39] E. Shaker, H. Mahmoud, S. Mnaa, Silymarin, the antioxidant component and Silybum marianum extracts prevent liver damage, Food Chem. Toxicol. 48(3) (2010) 803-6.
[40] A. Borah, R. Paul, S. Choudhury, A. Choudhury, B. Bhuyan, A.D. Talukdar, M.D. Choudhury, K.P. Mohanakumar, Neuroprotective potential of silymarin against CNS disorders: Insight into the pathways and molecular mechanisms of action, CNS Neurosci. Ther. 19(11) (2013) 847-853.
[41] S.K. Katiyar, Silymarin and skin cancer prevention: anti-inflammatory, antioxidant and immunomodulatory effects, Int. J. Oncol. 26(1) (2005) 169-176.
[42] A. Montgomery, T. Adeyeni, K. San, R.M. Heuertz, U.R. Ezekiel, Curcumin Sensitizes Silymarin to Exert Synergistic Anticancer Activity in Colon Cancer Cells, J. Cancer 7(10) (2016) 1250-7.
[43] A. Taleb, K.A. Ahmad, A.U. Ihsan, J. Qu, N. Lin, K. Hezam, N. Koju, L. Hui, D. Qilong, Antioxidant effects and mechanism of silymarin in oxidative stress induced cardiovascular diseases, Biomed. Pharmacother. 102 (2018) 689-698.
[44] H. Yu, M.-H. Nguyen, W.S. Cheow, K. Hadinoto, A new bioavailability enhancement strategy of curcumin via self-assembly nano-complexation of curcumin and bovine serum albumin, Materials Science and Engineering: C 75 (2017) 25-33.
[45] M. Reina, A. Martínez, Is silybin the best free radical scavenger compound in silymarin?, The Journal of Physical Chemistry B 120(20) (2016) 4568-4578.
[46] A.D. Boese, J.M. Martin, N.C. Handy, The role of the basis set: Assessing density functional theory, The Journal of chemical physics 119(6) (2003) 3005-3014.
[47] S. Thakurta, J. Chakraborty, G. Rosair, J. Tercero, M.S. El Fallah, E. Garribba, S. Mitra, Synthesis of two new linear trinuclear CuII complexes: Mechanism of magnetic coupling through hybrid B3LYP functional and CShM studies, lnorg. Chem. 47(14) (2008) 6227-6235.
[48] M. Frisch, G. Trucks, H. Schlegel, G. Scuseria, M. Robb, J. Cheeseman, V. Zakrzewski, J. Montgomery Jr, R.E. Stratmann, J. Burant, Gaussian 98, revision a. 7, Gaussian, Inc., Pittsburgh, PA 12 (1998).
[49] S. Plimpton, Fast Parallel Algorithms for Short-Range Molecular Dynamics, J. Comput. Phys. 117(1) (1995) 1-19.
[50] S.L. Mayo, B.D. Olafson, W.A. Goddard, DREIDING: a generic force field for molecular simulations, J. Phys. Chem. 94(26) (1990) 8897-8909.
[51] N.S. Mengke, B. Hu, Q.P. Han, Y.Y. Deng, M. Fang, D. Xie, A. Li, H.K. Zeng, Rapamycin inhibits lipopolysaccharide-induced neuroinflammation in vitro and in vivo, Mol. Med. Report. 14(6) (2016) 4957-4966.
[52] C. Nencini, G. Giorgi, L. Micheli, Protective effect of silymarin on oxidative stress in rat brain, Phytomedicine 14(2-3) (2007) 129-35.
[53] M.M. Bradford, A rapid and sensitive method for the quantitation of microgram quantities of protein utilizing the principle of protein-dye binding, Anal. Biochem. 72(1-2) (1976) 248-254.
[54] S. Genet, R.K. Kale, N.Z. Baquer, Alterations in antioxidant enzymes and oxidative damage in experimental diabetic rat tissues: effect of vanadate and fenugreek (Trigonella foenum graecum), Mol. Cell. Biochem. 236(1-2) (2002) 7-12.
[55] M. Khalkhali, S. Sadighian, K. Rostamizadeh, F. Khoeini, M. Naghibi, M. Hamidi, Simultaneous diagnosis and drug delivery by silymarin-loaded magnetic Nanoparticles, Nanomedicine Journal 2(3) (2015) 223-230.
[56] T. Chatterjee, A. Pal, S. Dey, B.K. Chatterjee, P. Chakrabarti, Interaction of virstatin with human serum albumin: spectroscopic analysis and molecular modeling, PLoS One 7(5) (2012) e37468.
[57] R. Fang, R. Hao, X. Wu, Q. Li, X. Leng, H. Jing, Bovine serum albumin nanoparticle promotes the stability of quercetin in simulated intestinal fluid, J. Agric. Food Chem. 59(11) (2011) 6292-6298.
[58] S.A. Soudi, M.I. Nounou, S.A. Sheweita, D.A. Ghareeb, L.K. Younis, L.K. El-Khordagui, Protective effect of surface-modified berberine nanoparticles against LPS-induced neurodegenerative changes: a preclinical study, Drug Deliv Transl Res (2019).

[59] a. rashidian, h. ghafari, m. chamanara, A. dehpour, a. muhammadnejad, r. akbarian, s.e. mousavi, S. Rezayat, The protective effect of nano-curcumin in experimental model of acute pancreatitis: The involvement of TLR4/NF-kB pathway, Nanomedicine Journal 5(3) (2018) 138-143.
[60] N. Fakhraei, S.E. Mousavi, S.P. Pishva, S.M. Rezayat, F. Mohammadi, Nanocurcumine Ameliorates Lipopolysaccharide-induced Depressive-like Behavior in Mice, (2018).
[61] P. Shukla, A.K. Verma, J. Dewangan, S.K. Rath, P.R. Mishra, Chitosan coated curcumin nanocrystals augment pharmacotherapy via improved pharmacokinetics and interplay of NFκB, Keap1 and Nrf2 expression in Gram negative sepsis, RSC Advances 5(70) (2015) 57006-57020.
[62] Z.E. Papay, A. Kosa, B. Boddi, Z. Merchant, I.Y. Saleem, M.G. Zariwala, I. Klebovich, S. Somavarapu, I. Antal, Study on the Pulmonary Delivery System of Apigenin-Loaded Albumin Nanocarriers with Antioxidant Activity, J. Aerosol Med. Pulm. Drug Deliv. 30(4) (2017) 274-288.
[63] P. Ghosh, A.S. Roy, S. Chaudhury, S.K. Jana, K. Chaudhury, S. Dasgupta, Preparation of albumin based nanoparticles for delivery of fisetin and evaluation of its cytotoxic activity, Int. J. Biol. Macromol. 86 (2016) 408-417.
[64] S. Das, P. Roy, R.G. Auddy, A. Mukherjee, Silymarin nanoparticle prevents paracetamol-induced hepatotoxicity, International journal of nanomedicine 6 (2011) 1291.
[65] K.Y. Yang, A.M.Y. Du Hyeong Hwang, D.W. Kim, Y.-J. Shin, O.-N. Bae, Y.-I. Kim, J.O. Kim, C.S. Yong, H.-G. Choi, Silymarin-loaded solid nanoparticles provide excellent hepatic protection: physicochemical characterization and in vivo evaluation, International journal of nanomedicine 8 (2013) 3333.
[66] N. Younis, M.A. Shaheen, M.H. Abdallah, Silymarin-loaded Eudragit® RS100 nanoparticles improved the ability of silymarin to resolve hepatic fibrosis in bile duct ligated rats, Biomed. Pharmacother. 81 (2016) 93-103.
[67] W.-C. Hsu, L.-T. Ng, T.-H. Wu, L.-T. Lin, F.-L. Yen, C.-C. Lin, Characteristics and antioxidant activities of silymarin nanoparticles, Journal of nanoscience and nanotechnology 12(3) (2012) 2022-2027.
[68] M. Shangguan, Y. Lu, J. Qi, J. Han, Z. Tian, Y. Xie, F. Hu, H. Yuan, W. Wu, Binary lipids-based nanostructured lipid carriers for improved oral bioavailability of silymarin, J. Biomater. Appl. 28(6) (2014) 887-96.
[69] S.A. Guhagarkar, D. Shah, M.D. Patel, S.S. Sathaye, P.V. Devarajan, Polyethylene sebacate-Silymarin nanoparticles with enhanced hepatoprotective activity, Journal of nanoscience and nanotechnology 15(6) (2015) 4090-4093.
[70] M. Cengiz, H.M. Kutlu, D.D. Burukoglu, A. Ayhancı, A comparative study on the therapeutic effects of silymarin and silymarin-loaded solid lipid nanoparticles on d-GaIN/TNF-α-induced liver damage in balb/c mice, Food Chem. Toxicol. 77 (2015) 93-100.
[71] Y. Ma, S. He, X. Ma, T. Hong, Z. Li, K. Park, W. Wang, Silymarin-loaded nanoparticles based on stearic acid-modified Bletilla striata polysaccharide for hepatic targeting, Molecules 21(3) (2016) 265.
[72] M.A. Abdel-Wahhab, A.A. El-Nekeety, A.S. Salman, S.H. Abdel-Aziem, F.M. Mehaya, N.S. Hassan, Protective capabilities of silymarin and inulin nanoparticles against hepatic oxidative stress, genotoxicity and cytotoxicity of Deoxynivalenol in rats, Toxicon 142 (2018) 1-13.
[73] J. Liang, Y. Liu, J. Liu, Z. Li, Q. Fan, Z. Jiang, F. Yan, Z. Wang, P. Huang, N. Feng, Chitosan-functionalized lipid-polymer hybrid nanoparticles for oral delivery of silymarin and enhanced lipid-lowering effect in NAFLD, Journal of nanobiotechnology 16(1) (2018) 64.
[74] A. Ashraf, P.A. Mahmoud, H. Reda, S. Mansour, M.H. Helal, H.E. Michel, M. Nasr, Silymarin and silymarin nanoparticles guard against chronic unpredictable mild stress induced depressive-like behavior in mice: involvement of neurogenesis and NLRP3 inflammasome, J. Psychopharm. (2019) 0269881119836221.

[75] Cristofalo R, Bannwart-Castro CF, Magalhaes CG, Borges VT, Peracoli JC, Witkin SS, Peracoli MT. Silibinin attenuates oxidative metabolism and cytokine production by monocytes from preeclamptic women. Free Radic Res. 2013;47(4):268-75.

[76] Taleb A, Ahmad KA, Ihsan AU, Qu J, Lin N, Hezam K, Koju N, Hui L, Qilong D. Antioxidant effects and mechanism of silymarin in oxidative stress induced cardiovascular diseases. Biomed Pharmacother. 2018;102:689-98.

[77] Zhu SY, Dong Y, Tu J, Zhou Y, Zhou XH, Xu B. Silybum marianum oil attenuates oxidative stress and ameliorates mitochondrial dysfunction in mice treated with D-galactose. Pharmacogn Mag. 2014;10(Suppl 1):S92-9.

[78] Khazim K, Gorin Y, Cavaglieri RC, Abboud HE, Fanti P. The antioxidant silybin prevents high glucose-induced oxidative stress and podocyte injury in vitro and in vivo. Am J Physiol Renal Physiol. 2013;305(5):F691-700.

[79] Surai PF. Silymarin as a Natural Antioxidant: An Overview of the Current Evidence and Perspectives. Antioxidants (Basel, Switzerland). 2015;4(1):204-47.

[80] Zhao X, Deng Y, Zhang Y, Zu Y, Lian B, Wu M, Zu C, Wu W. Silymarin nanoparticles through emulsion solvent evaporation method for oral delivery with high antioxidant activities, bioavailability, and absorption in the liver. RSC Advances. 2016;6(95):93137-46.

[81] Abdel-Wahhab MA, El-Nekeety AA, Salman AS, Abdel-Aziem SH, Mehaya FM, Hassan NS. Protective capabilities of silymarin and inulin nanoparticles against hepatic oxidative stress, genotoxicity and cytotoxicity of Deoxynivalenol in rats. Toxicon. 2018;142:1-13.

[82] Ashraf A, Mahmoud PA, Reda H, Mansour S, Helal MH, Michel HE, Nasr M. Silymarin and silymarin nanoparticles guard against chronic unpredictable mild stress induced depressive-like behavior in mice: involvement of neurogenesis and NLRP3 inflammasome. J Psychopharm. 2019;33(5):615-31.

Graphical abstract

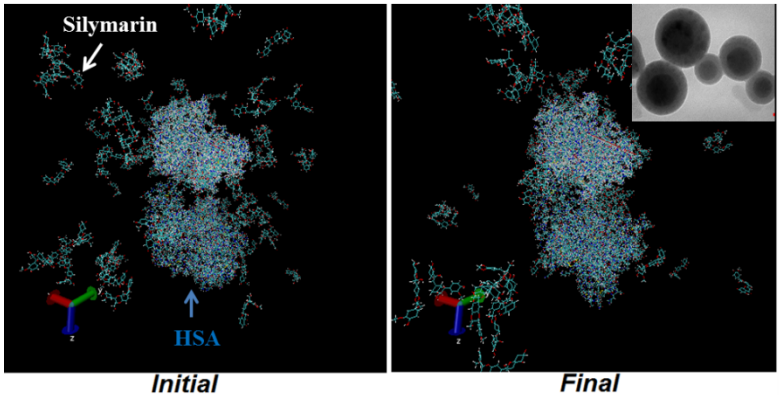

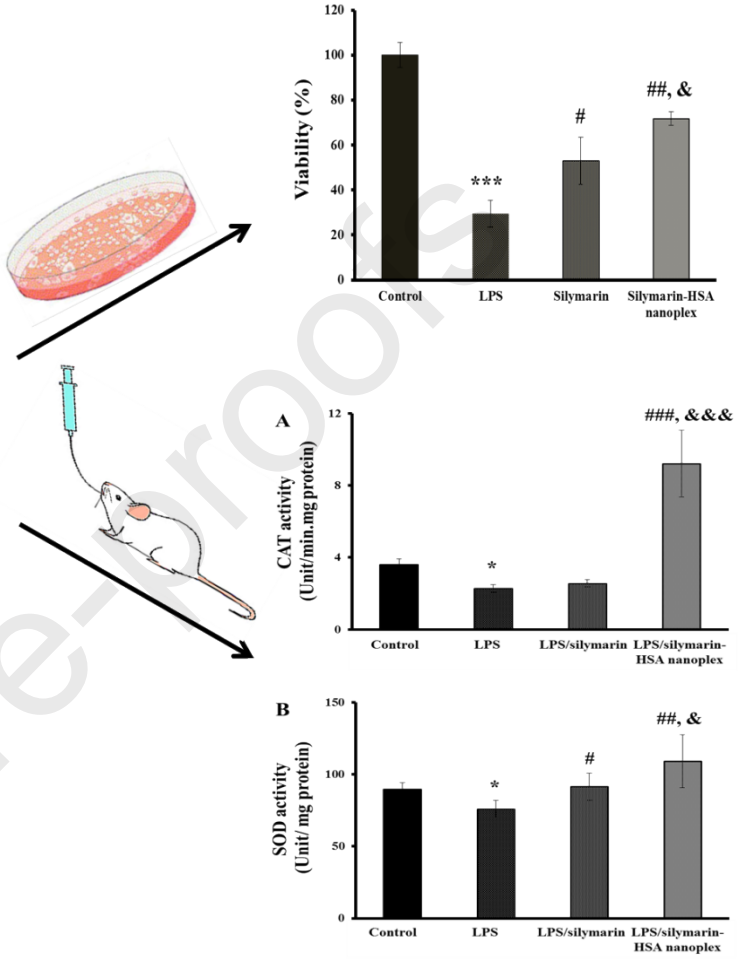

Conflict of interest

The authors declare no conflict of interest